Fuel 300 (2021) 120979

Contents lists available at ScienceDirect

Fuel

journal homepage: www.elsevier.com/locate/fuel

Full Length Article

Study of the oxidation of ammonia in a flow reactor. Experiments and kinetic modeling simulation

M. Abián, M. Benés, A. de Goñi, B. Muñoz, M.U. Alzueta *

Aragón Institute of Engineering Research (I3A), Department of Chemical and Environmental Engineering, University of Zaragoza, 50018 Zaragoza, Spain

ARTICLE INFO

Keywords:
Ammonia
Oxidation
Nitrogen oxides
Kinetic modeling
Carbon-free fuels

ABSTRACT

The present work is focused on the analysis of the ammonia oxidation process and the formation of main nitrogen oxides (NO, NO_2 and N_2O) over a wide range of temperatures and O_2 reaction environments. Experiments are performed at atmospheric pressure in a laboratory quartz tubular flow reactor, covering the temperature range of 875 to 1450 K and for different air excess ratios (from pyrolysis to very oxidizing conditions). The experimental results are simulated and interpreted in terms of a detailed chemical-kinetic mechanism. Reaction path and sensitivity analyses are used to delineate the NH_3 oxidation scheme.

1. Introduction

Combustion of carbonaceous fossil fuels is considered as one of the main responsible of the emission to the atmosphere of greenhouse CO_2 gas and important atmospheric pollutants, such as soot. To go towards a decarbonisation of energy, ammonia has been identified as a promising fuel for transport and power applications [1–3]. Besides technical aspects on NH_3 utilization, a key issue is its proper combustion in relation to the minimization of NO_x and NH_3 emissions in the flue gases. Therefore, the successful application of NH_3 as an alternative transportation fuel should be grounded on the deep understanding of its combustion characteristics [4].

Literature works on ammonia oxidation include studies in flames [4–9], shock tubes [10–12], rapid compression machines [13], jet-stirred reactors [14,15] and flow reactors [14,16,17]; covering thus a wide range of operating conditions for ammonia conversion process characterization.

During its oxidation, NH_3 may be converted to nitrogen oxides or to N_2, depending on the operating conditions [18]. Song et al. [17] carried out a study of the conversion of ammonia at high pressure (up to 100 bar), in the 450–925 K temperature range and for fuel-lean conditions, and found that the main nitrogen products formed were N_2 and N_2O. They did not find NO nor NO_2. Skreiberg et al. [16] performed a modeling study of the oxidation process of NH_3, based on flow reactor measurements at atmospheric pressure and fuel-rich conditions by Hasegawa and Sato [19]. They stressed up the attention in NO behavior, with no mention to NO_2 or N_2O, which points to NO as the main nitrogen oxide under these conditions. Stagni et al. [15] also identified NO as the main nitrogen oxide formed in jet-stirred and tubular flow reactors at fuel-lean conditions. Shu et al. [12] observed from the ammonia/air shock tube analysis at intermediate temperatures (1100–1600 K) and relatively high pressures (20 and 40 bar) that the ammonia combustion could be potentially free from NO_x and NH_3 emissions at fuel-rich conditions.

In parallel with the experimental advances on this topic, considerable progress has been achieve on developing a chemical kinetic mechanism for modeling the ammonia combustion process, and currently, there are available in the literature a considerable number of chemical kinetic mechanisms [11,20–25]. Recently, Dai et al. [26] have evaluated four NH_3 oxidation mechanisms: the mechanisms from Klippenstein et al. (2011) [24], Mathieu and Petersen (2015) [11], Shrestha et al. (2018) [25], and a new version of the mechanism described by Glarborg et al. (2018) [23], updated in relation to the rate constant for the formation of hydrazine, $NH_2 + NH_2 (+M) = N_2H_4 (+M)$, in their present work. The authors concluded that, in general, the updated Glarborg et al. mechanism [23] showed the best performance, yielding satisfactory prediction of ignition delay times both of pure NH_3 and NH_3/H_2 mixtures at high pressures (40–60 bar). For this reason, this mechanism has been chosen for simulations in the present work.

In this context, to extend the knowledge on the NH_3 conversion process under combustion conditions (from pyrolysis to very oxidizing conditions), the present study accomplishes an experimental study of NH_3 conversion and formation of main nitrogen oxides (NO, NO_2 and N_2O), in a quartz tubular flow reactor, at atmospheric pressure, over the

* Corresponding author.
E-mail address: uxue@unizar.es (M.U. Alzueta).

https://doi.org/10.1016/j.fuel.2021.120979
Received 1 March 2021; Received in revised form 21 April 2021; Accepted 2 May 2021
Available online 10 May 2021

875 to 1450 K temperature range and for different air excess ratios. The experimental results of the present work are simulated and interpreted by using the Glarborg et al. mechanism [23] with minor updates present work [27], both to extend the test conditions for the characterization of the performance of this mechanism and to highlight the most influencing reactions in the NH_3 oxidation process. Additionally, this analysis is used to suggest new updates for model refinements.

2. Experimental methodology

The experiments are performed at atmospheric pressure in an experimental installation previously used by the group to study the gas-phase oxidation process of different compounds [28,29]. Fig. 1 shows a scheme of the experimental installation.

Reactants, and nitrogen to balance, are fed from gas cylinders (provider: Air Liquide or Praxair) through mass flow controllers. The gas cylinders contained high-purity gases with a relative uncertainty of 3% determined for a confidence interval of 95%. The gases are fed to the quartz tubular flow reactor in four separate streams, following the procedure of Alzueta et al. [30] and mixed in cross flow at the inlet of the reaction zone. This reaction zone has 20 cm in length and 0.87 cm of inside diameter. The reactor is placed in a three-zone electrically heated oven, ensuring an isothermal reaction zone (±5 K). Just after the reaction zone, the reactor has an external air fed cooling jacket to cool down the product gas. The total flow rate in the experiments is 1 L (STP)/min, which gives a temperature dependent gas residence time in the isothermal reaction zone of tr(s) = 195/T(K). Fig. 2 shows the temperature profiles obtained for different temperatures along the reaction zone. The uncertainty of the type K thermocouple used for measurements is estimated as ± 1.5 K

Downstream the reactor, the product gas is directed to: i) a gas micro-chromatograph (*Agilent Technologies*) equipped with thermal conductivity detectors (TCD), which has been calibrated with high-purity gases for NH_3, O_2, H_2 and N_2O quantification, ii) a continuous infrared NO analyzer (*ABB, model: advance optima*) and, iii) a chemiluminescence NO_x (NO and NO_2) analyzer equipped with a catalytic converter (*Eco-Physics*). Therefore, the joint use of these measuring equipment has allowed the quantification of NH_3, O_2, H_2, N_2O, NO and NO_2, with an estimated uncertainty of the measurements within ± 5%, but not less than 5 ppm for the continuous analyzers and not less than 10 ppm for the gas micro-chromatograph. Since the experiments have been performed using N_2 as bulk gas, and given the ammonia diluted conditions (nominal concentration of 0.1%), molecular nitrogen formed from ammonia reaction is negligible compared with the total N_2, making not possible to quantify the fraction of NH_3 converted into N_2.

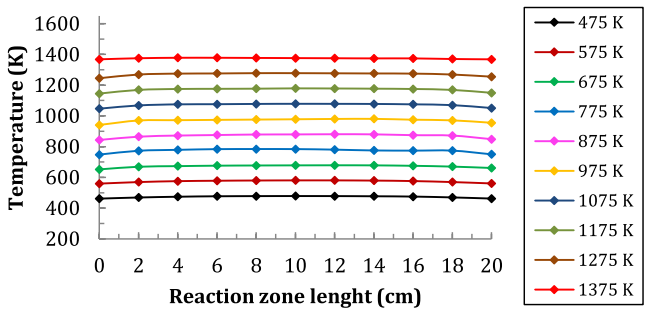

Fig. 2. Temperature profiles within the reaction zone of the tubular flow reactor.

Table 1 shows the conditions of the test cases. A nominal concentration of 0.1% NH_3 has been introduced in all the experiments, and the amount of O_2 has varied from pyrolysis ($\lambda = 0$) to very fuel-lean conditions ($\lambda = 22$). The air excess ratio, λ, used to characterize the oxygen environment has been determined considering the stoichiometry of the reaction $NH_3 + 0.75\ O_2 \rightleftharpoons 0.5\ N_2 + 1.5\ H_2O$. Sets 4 and 5 are repeated experiments over the NH_3 conversion temperature range at stoichiometric conditions (results included in Fig. 4)

3. Chemical-kinetic modeling

In order to go further into the understanding of the ammonia conversion process, the present experimental results are simulated and interpreted in terms of the mechanism described by Glarborg et al. [23], with minor updates included in the study of CH_3CN conversion [27], only related to the CH_3CN reaction subset, and including the interaction of NH_3 and NH_2 to produce N_2H_3 and H_2 (reaction r.1), as described in the work of Dove and Nip [31],

$$NH_3 + NH_2 \rightleftharpoons N_2H_3 + H_2 \qquad \text{(r.1)}$$

This reaction was shown to be necessary in earlier studies of ammonia thermal decomposition by Konnov and De Ruyck (2000) [32] using the experimental shock wave data under pyrolysis conditions of Davinson et al. [33]. While Konnov and De Ruyck [32] used for this reaction the value of $1.0{\cdot}10^{11}T^{0.5}\exp(-21600/RT)$, slightly lower than the original determination of Dove and Nip [31] of $8.0{\cdot}10^{11}T^{0.5}\exp(-21600/RT)$, we have adopted the original recommendation by Dove and Nip. As will be seen later, this reaction exhibits an important effect

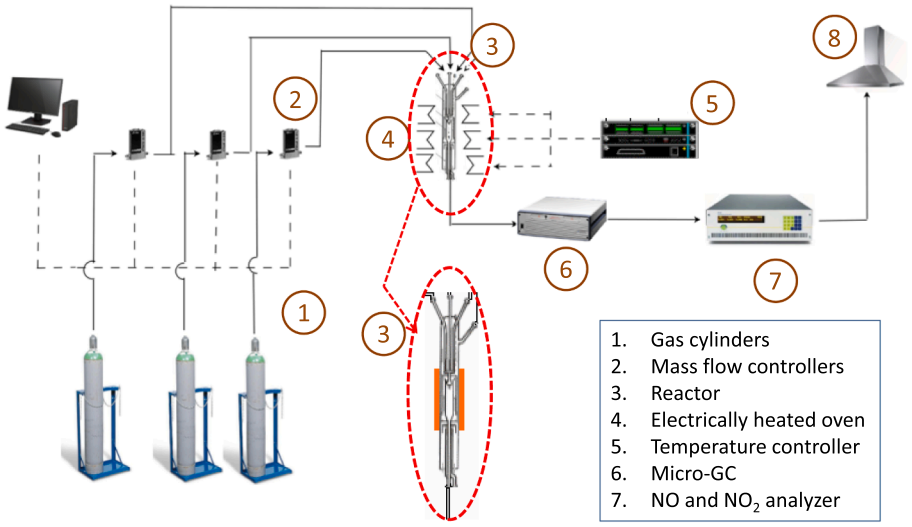

Fig. 1. Experimental installation.

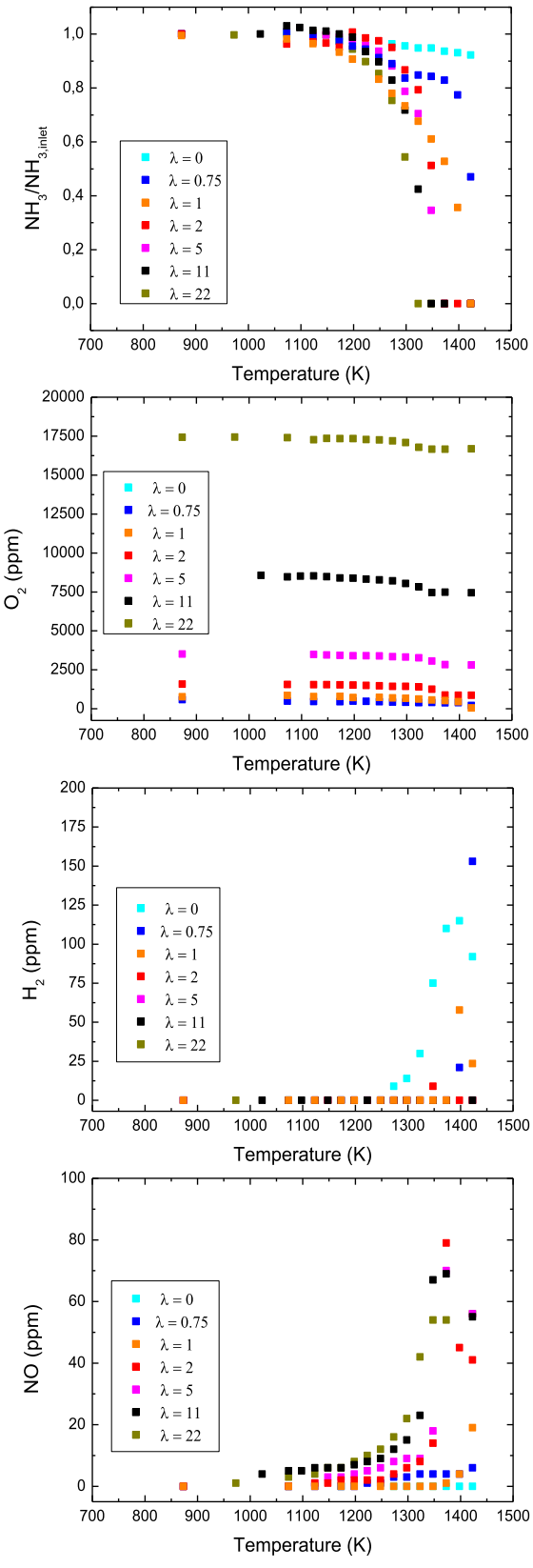

Fig. 3. Conversion of NH_3 and concentration results of O_2, H_2 and NO as a function of the reaction temperature for λ = 0 to λ = 22. Inlet concentrations correspond to sets 1, 3, 4 and 6–9 in Table 1.

Table 1
Matrix of experimental conditions. All experiments are performed at atmospheric pressure in the 875–1450 K temperature range, with a total flow rate of 1 L (STP)/min and using N_2 as bath gas. [x]The air excess ratio (λ) is determined considering the stoichiometry of reaction: $NH_3 + 0.75\ O_2 \rightleftharpoons 0.5\ N_2 + 1.5\ H_2O$. tr (s) = 195/T(K).

Set	NH_3 (ppm)	O_2 (ppm)	H_2O(%)	λ^x
1	1149	0	0	0
2	971	298	0	0.4
3	1033	579	0	0.75
4	976	780	0	1
5	926	794	0	1
6	990	1576	0	2
7	885	3517	0	5
8	1055	8861	0	11
9	1025	16,882	0	22
10	969	823	0.3	1

on the simulation predictions, and thus a more precise re-evaluation of the present rate would be desirable. The thermodynamic data used are taken from the same sources as the kinetic mechanisms. Apart from including reaction r1, the reaction mechanism used in the present work includes submechanisms for C1-C2 hydrocarbons [34–36], amines [37], cyanides [38] and hydrocarbon/nitrogen interactions [39–41].

The modeling study has been carried out using the plug-flow reactor (PFR) model of the Chemkin Pro suite [42], using a "fix gas temperature" problem type using the experimentally temperature shown in Fig. 2. The rest of initial operating conditions are those of Table 1. Similar results are obtained using the "closed homogenous reactor" model.

4. Results and discussion

To evaluate the influence of air excess ratio (λ) on the NH_3 oxidation process, Fig. 3 shows the conversion of NH_3 and O_2 and the formation of H_2 and NO (ppm) as function of the reaction temperature and for λ = 0, 0.75, 1, 2, 5, 11 and 22.

These results indicate that the oxygen availability is a key factor in the process. The higher the O_2 level in the reaction environment, the lower the temperature necessary for the complete conversion of NH_3. However, the excess of O_2 favors the formation of NO, as compared with low oxygen levels. The maximum yield to NO (eq.1) is attained at around 1375 K for oxidizing conditions (λ ≥ 5), with a value of around 7%. H_2 was only detected for λ ≤ 2, and it shows an increasing concentration tendency when the oxygen concentration decreases.

$$NO_{yield}(\%) = 100^{*}[NO]_{outlet}/[NH_3]_{inlet} \quad (1)$$

Table 2 summarizes the temperature intervals for the 10, 50 and 100% conversion of NH_3. Whereas the onset temperature for NH_3 conversion is not clearly affected by the oxygen environment, both the 50 and 100% NH_3 conversion temperatures are shifted to higher values as the oxygen availability is decreased, which originates a widening of the temperature window for NH_3 conversion. Under pyrolysis (λ = 0) and reducing conditions (λ = 0.75), NH_3 is not fully consumed in the temperature interval considered in this work.

Fig. 4 shows an example of the repeatability of the experiments for a stoichiometry of 1. Results indicate the good reproducibility of the experiments. Additionally, results of NH_3 oxidation at stoichiometric conditions in the absence and presence of 0.3% H_2O are also shown in Fig. 4 (set 10). NH_3 and O_2 start their conversion at approximately 1200 K for both dry and wet NH_3 oxidation. The negligible effect of water vapor presence, in particular at the onset of reaction and in general over the whole temperature regime is an indication of the non-occurrence of significant wall catalytic reactions under the studied conditions, which have been reported to may be appreciable when evaluating NH_3 oxidation [14,23]. Also, the recent results by our group [43] on the

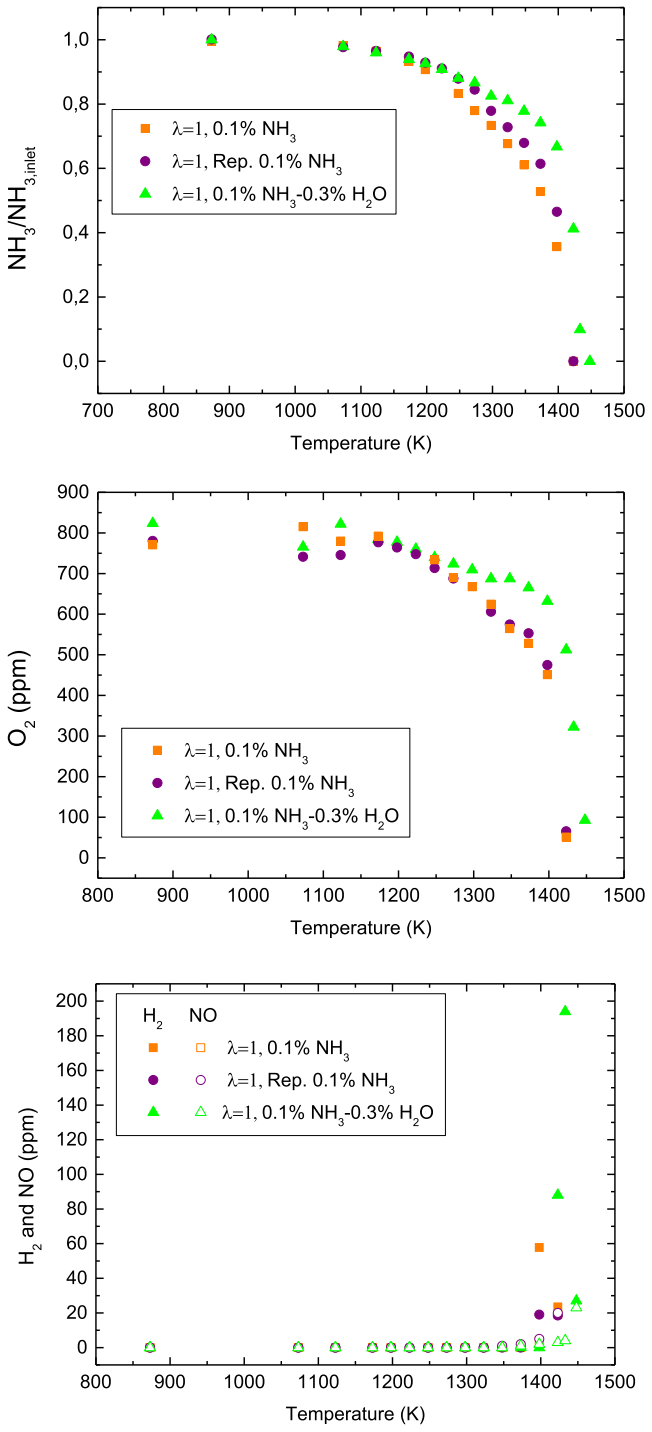

Fig. 4. Conversion of NH_3 and concentration results of O_2, H_2 and NO as a function of the reaction temperature for $\lambda = 1$ in both the absence and presence of H_2O. Inlet concentrations correspond to sets 4, 5 and 10 in Table 1.

pyrolysis of ammonia in different flow reactors of either quartz and non-porous alumina did not show as significant the effect of surfaces for ammonia conversion. In addition to N_2 (not measured since N_2 is also used as dilution gas), NO is the main nitrogen product from NH_3 oxidation. Neither NO_2 nor N_2O were detected under any of the conditions analyzed in this work. The conversion of NH_3 also results in the formation of H_2, which concentration is considerably increased in the presence of H_2O. As NO, H_2 was produced only at the highest temperatures considered (≥1400 K).

Fig. 5 compares experimental and modeling results, with the above

Table 2
Temperature intervals for the 10, 50 and 100% NH_3 conversion as a function of air excess ratio (λ).

λ	$T_{10\%ConvNH3}$(K)	$T_{50\%ConvNH3}$(K)	$T_{100\%ConvNH3}$(K)
0	> 1423	–	–
0.75	1248–1273	1398–1423	–
1	1198–1248	1373–1398	1398–1423
2	1273–1298	1323–1348	1348–1373
5	1248–1273	1323–1348	1348–1373
11	1223–1248	1298–1323	1323–1348
22	1198–1223	1273–1298	1298–1323

reported mechanism (section 3, chemical-kinetic modelling), for the conversion of NH_3 and the formation of H_2 and NO, as a function of temperature and for selected stoichiometries: $\lambda = 0.4$, 1, 2, 5,11 and 22. Symbols represent experimental data and lines indicate model predictions.

As can be observed in Fig. 5, despite some differences between experimental results and simulations, the model is able, in general, to reproduce the main features of NH_3 conversion as a function of temperature. However, while the onset of NH_3 conversion is reasonably predicted, the full conversion of this species is predicted to occur at a lower temperature compared to the experimental findings. This results in a shift of the prediction of H_2 and NO formation.

Sensitivity analyses were performed to identify the most important reactions controlling the conversion of NH_3 at atmospheric pressure and flow reactor conditions.

Fig. 6 shows normalized sensitivity coefficients for initiation NH_3 conversion, i.e. when calculated NH_3 has reached a conversion of approximately 1 ppm, in the experiments corresponding to sets 2 ($\lambda = 0.4$), 4 ($\lambda = 1$) and 8 ($\lambda = 11$) in Table 1.

In Fig. 6, the sensitivity analysis for NH_3 conversion shows the reaction (r.1) as the most sensitive one, regardless of the stoichiometry considered.

The negative sensitivity coefficient of reaction 1 indicates a promoting effect of NH_3 consumption, if its rate constant is increased. As indicated in the chemical-kinetic modeling section (section 3), under pyrolysis conditions, the amine radicals formed from NH_3 conversion may potentially interact with the unreacted ammonia, generating higher amines [31], i.e. through reaction r.1.

Amine species, and their interactions, were also found to dominate the kinetics of ammonia rich flames [44], while they were insignificant under stoichiometric and lean flame conditions [45].

Konnov and De Ruyck [32] developed a reaction mechanism for the thermal decomposition of ammonia and validated it against experimental data of ammonia pyrolysis in shock waves by Davidson et al. (1990) [33]. Originally, the authors adopted the rate constant of the reaction r.1 ($8.0{\cdot}10^{11}T^{0.5}\exp(-21600/RT)$; *units: cal, cm³, mol, s*) given by Dove and Nip [31]. However, the authors observed that with this value the mechanism overestimated the NH concentration, and underestimated the times-to-peak for both NH_2 and NH radicals, especially in mixtures with higher ammonia contents. To overcome this issue, Konnov and De Ruyck [32] proposed a new value for this reaction ($1.0{\cdot}10^{11}T^{0.5}\exp(-21600/RT)$; *units: cal, cm³, mol, s*), that improved significantly the simulation of the Davison et al. [33] data.

To contribute to elucidate the role of reaction $NH_3 + NH_2 \rightleftharpoons N_2H_3 + H_2$ (r.1) in the ammonia combustion process, in the present work, a study of the impact of the presence of that reaction has been made, using both the mechanism used for simulations in the present work (see section 3) [23,27] and the recently published mechanism of Stagni et al. [15] validated for fuel-lean NH_3 conversion in perfect stirred and plug-flow reactors. It is worth to highlight that neither of the original mechanisms [15,23–27] included this reaction within their respective amine subset, and thus, the test also includes the modeling results without this reactions. Additionally, both the original value of the constant for reaction r1 by Dove and Nip [31] and the modified value by

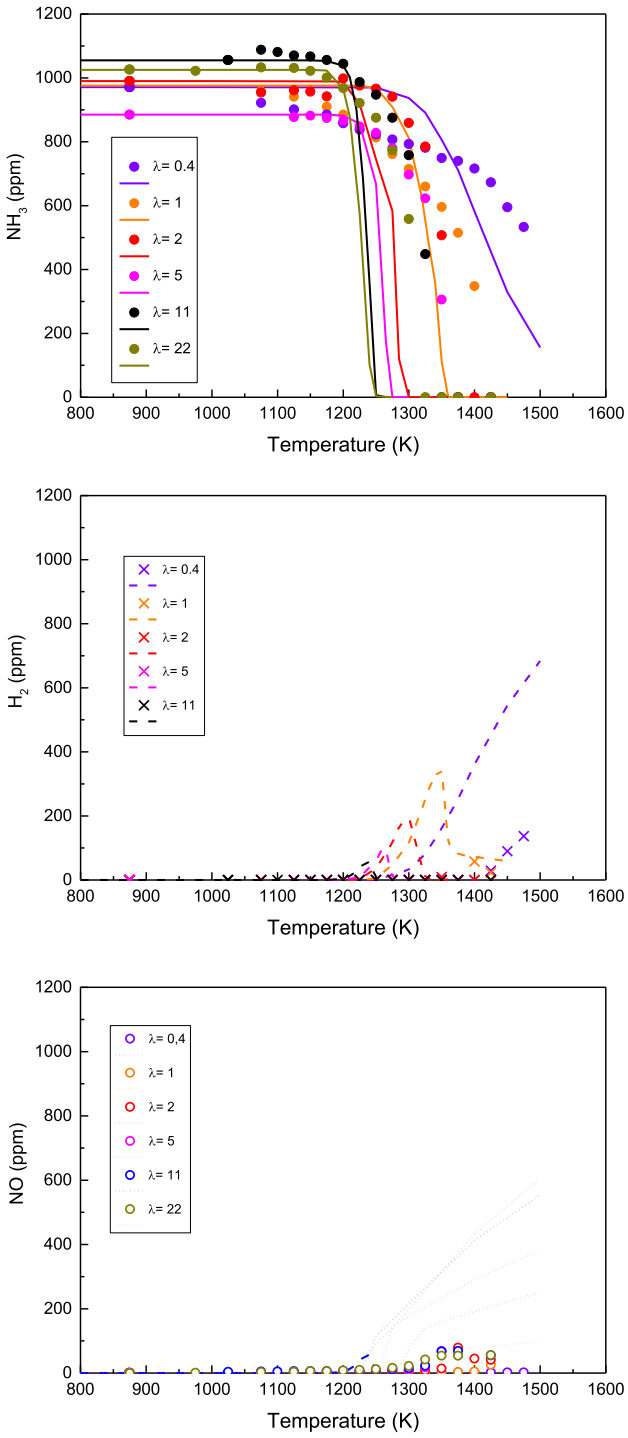

Fig. 5. Comparison of experimental data and modeling predictions for concentrations of NH_3, H_2 and NO as a function of temperature and for selected stoichiometries ($\lambda = 0.4$, 1, 2, 5, 11 and 22). Inlet concentrations correspond to sets 2, 4, 6, 7, 8 and 9 in Table 1.

Konnov and De Ruyck [32] were tested. Fig. 7 shows the comparison of the modeling predictions with experimental data on ammonia conversion under selected stoichiometric conditions, $\lambda = 1$ (set 4 in Table 1).

The comparison in Fig. 7 shows that the NH_3 conversion profile is predicted more accurately when including reaction r.1 in both mechanisms, otherwise both mechanisms predict the oxidation of ammonia to occur at much higher temperatures than observed experimentally. The modeling results are also highly influenced by the specific rate constant values considered for reaction r1. A decrease of a factor of 8 from the

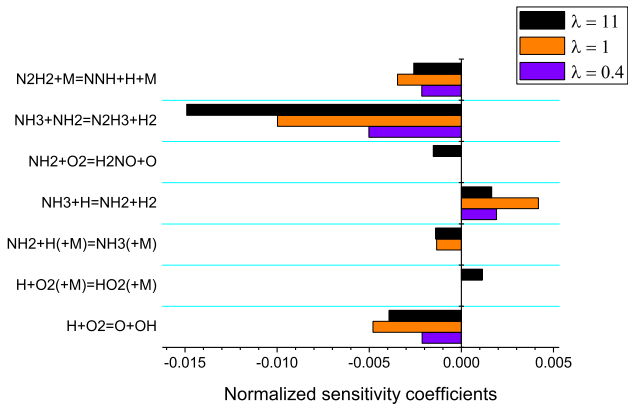

Fig. 6. Sensitivity analysis for NH_3 conversion at: $\lambda = 0.4$ and 1250 K; $\lambda = 1$ and 1225 K; $\lambda = 11$ and 1175 K.

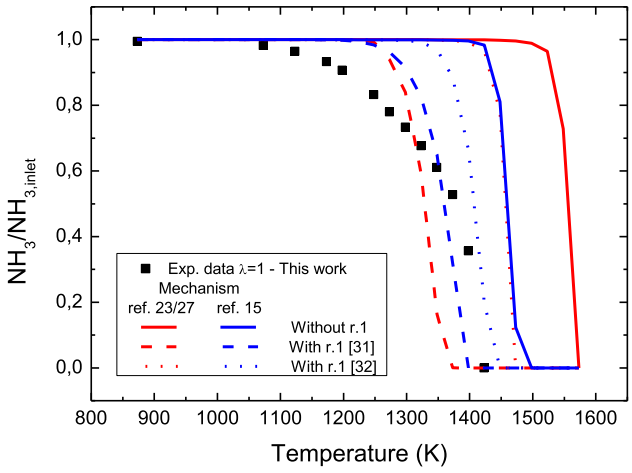

Fig. 7. Comparison of experimental (present work) and predicted conversion results of NH_3 using different mechanism configurations, as a function of temperature. Lines denote model predictions obtained with different values for the rate constant of the $NH_3 + NH_2 \rightleftharpoons N_2H_3 + H_2$ reaction (r.1). The inlet conditions correspond to set 4 in Table 1.

original determination of the Dove and Nip [31] value to the value used by Konnov and De Ruyck [32], exhibits a significant difference in the simulated results. This, together with the sensitivity analysis carried out in the present work, indicates the importance of reaction r1, and reinforces the necessity for a more precise determination of their kinetic parameters.

Fig. 8 includes a reaction pathway diagram for the oxidation of NH_3 including conditions ranging from fuel-rich to fuel-lean ones. At the beginning of reaction, NH_3 is decomposed through reaction (r.2). Once the process is initiated, thermal decomposition (r.2) becomes of secondary importance, and NH_3 is converted to NH_2 by reaction with OH, O and H radicals (r.3-r.5), primarily OH., and to N_2H_3 (r.1) by reaction with the NH_2 formed.

$$NH_3(+M) \rightleftharpoons NH_2 + H\ (+M) \quad \text{(r.2)}$$

$$NH_3 + OH \rightleftharpoons NH_2 + H_2O \quad \text{(r.3)}$$

$$NH_3 + O \rightleftharpoons NH_2 + OH \quad \text{(r.4)}$$

$$NH_3 + H \rightleftharpoons NH_2 + H_2 \quad \text{(r.5)}$$

$$NH_3 + NH_2 \rightleftharpoons N_2H_3 + H_2 \quad \text{(r.1)}$$

The NH_2 radicals may follow two different but interconnected

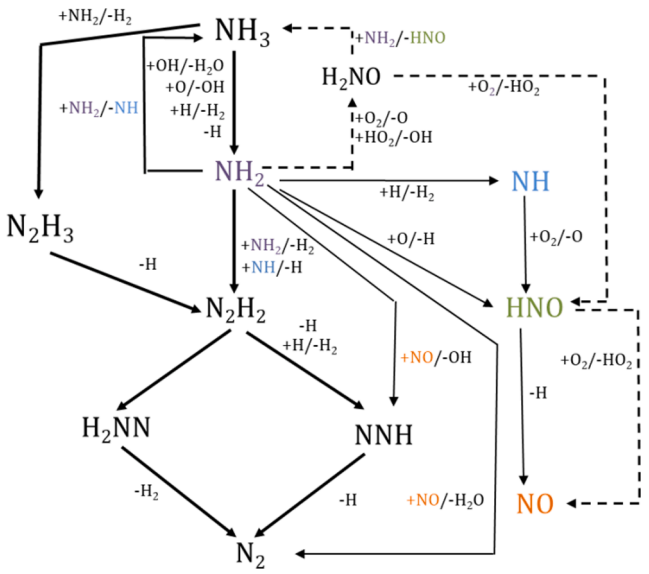

Fig. 8. Reaction path diagram for the oxidation of NH_3 under different stoichiometry conditions, ranging from fuel-rich to fuel-lean. Dashed lines denote reactions only important under fuel-lean conditions. Thickness of the arrows indicates the qualitative importance of pathways.

reaction schemes, leading, respectively, to the formation of NO and N_2. Interaction of NH_2 with H and O radicals leads to the formation of HNO (reaction sequence r.6-r.7 ($NH_2 \rightarrow NH \rightarrow HNO$), followed by reaction r.8) and subsequently to NO (r.9).

$$NH_2 + H \rightleftharpoons NH + H_2 \quad \text{(r.6)}$$

$$NH + O_2 \rightleftharpoons HNO + O \quad \text{(r.7)}$$

$$NH_2 + O \rightleftharpoons HNO + H \quad \text{(r.8)}$$

Interaction of NH_2 with nitrogen containing compounds (i.e. NH_3, NH_2, NH and NO) leads to the formation of N_2. In particular, the formation of N_2 from the interaction of NH_2 with nitrogen containing compounds other than NO takes place through the formation of N_2H_2 as intermediate amine specie, (reaction sequences involving reactions r.1, r.9 to r.16),

$$NH_3 + NH_2 \rightleftharpoons N_2H_3 + H_2 \quad \text{(r.1)}$$

$$N_2H_3 \rightleftharpoons N_2H_2 + H \quad \text{(r.9)}$$

$$NH_2 + NH_2 \rightleftharpoons N_2H_2 + H_2 \quad \text{(r.10)}$$

$$NH_2 + NH \rightleftharpoons N_2H_2 + H \quad \text{(r.11)}$$

$$N_2H_2 \rightleftharpoons H_2NN \quad \text{(r.12)}$$

$$N_2H_2 \rightleftharpoons NNH + H \quad \text{(r.13)}$$

$$N_2H_2 + H \rightleftharpoons NNH + H_2 \quad \text{(r.14)}$$

$$H_2NN \rightleftharpoons N_2 + H_2 \quad \text{(r.15)}$$

$NNH \rightleftharpoons N_2 + H$ (r.16),

whereas the formation of N_2 from the interaction of NH_2 with NO takes place through a more direct route (reaction sequence involving reactions r.18 and r.16 and reaction r.19).

$$NH_2 + NO \rightleftharpoons NNH + OH \quad \text{(r.18)}$$

$$NH_2 + NO \rightleftharpoons N_2 + H \quad \text{(r.19)}$$

Under oxidizing conditions, new reaction pathways leading to the formation of nitroxide (H_2NO) are activated (r.20 and r.21).

$$NH_2 + HO_2 \rightleftharpoons H_2NO + OH \quad \text{(r.20)}$$

$$NH_2 + O_2 \rightleftharpoons H_2NO + O \quad \text{(r.21)}$$

Subsequently, H_2NO reacts with O_2 and NH_2 to form HNO (r.22 and r.23), which, in turn reacts with O_2 leading to the net formation of NO (r.24).

$$H_2NO + O_2 \rightleftharpoons HNO + HO_2 \quad \text{(r.22)}$$

$$H_2NO + NH_2 \rightleftharpoons NH_3 + HNO \quad \text{(r.23)}$$

$$HNO + O_2 \rightleftharpoons NO + HO_2 \quad \text{(r.24)}$$

Normalized sensitivity coefficients for NO concentration formed in the oxidation of NH_3 for the conditions of sets 3 ($\lambda = 1$) and 9 ($\lambda = 22$) in Table 1 are shown in Fig. 9. The analysis shows that the reactions of importance for NO formation depend on the λ value considered. For stoichiometric conditions, the formation of NO is sensitive to reactions involving N_2H_x and NH_x, and it is noticeable the comparatively high relevance of the $NH_3 + NH_2 = N_2H_3 + H_2$ reaction for both conditions considered. Under very fuel-lean conditions, the formation of NO is also sensitive to the H_2NO reaction subset, in particular to the reaction of NH_2 with O_2 to form H_2NO and O. Discrepancies between experimental and modeling predictions of NO formation, which are more important as the stoichiometry is increased (Fig. 4) may arise from chemistry involving H_2NO, since, as it was pointed out by Glarborg et al. [23] in the source paper of the used mechanism: "the H_2NO subset is not well stablished and consists largely of reactions with estimated rate constants".

5. Conclusions

An experimental study of the conversion of NH_3 and the formation of main nitrogen oxides has been performed in a quartz tubular flow reactor, at atmospheric pressure and in the 875–1450 K temperature range. Different stoichiometries were considered (λ = 0 to 22) and the results of the tests performed were interpreted in term of a detailed chemical-kinetic mechanism.

Experimental results indicate that the oxygen availability is a key factor in the process. The higher the O_2 level in the reaction environment, the lower the temperature necessary for the complete conversion of NH_3. However, the excess of O_2 favors the formation of NO compared to reducing conditions. Nor NO_2 neither N_2O were quantified at any of the conditions of the present work.

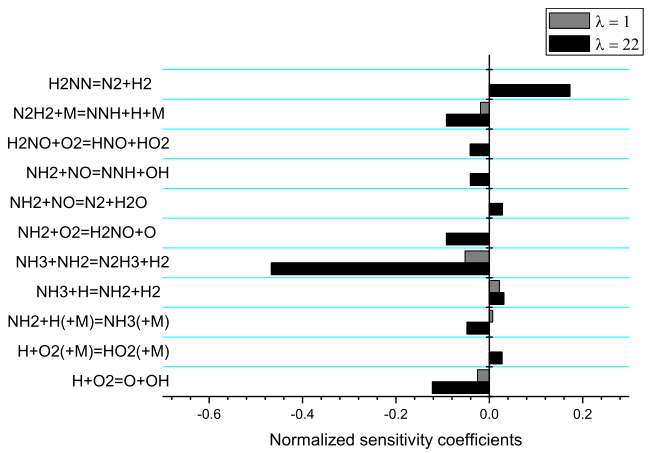

Fig. 9. Sensitivity coefficients for prediction of NO in the oxidation of NH_3, for $\lambda = 1$ and 22, at a temperature slightly above the temperature for onset of NH_3 conversion: $\lambda = 1$ (1250 K) and $\lambda = 22$ (1150 K).

The mechanism used to interpret the experimental results is able to describe the main trends of the conversion of NH_3 under the studies conditions, even though it overpredicts conversion of ammonia at high temperatures and formation of H_2 and NO. Reaction path and sensitivity analyses point to the interaction of amine species and H_2NO chemistry as key factors in the process.

CRediT authorship contribution statement

M. Abián: Conceptualization, Methodology, Writing - review & editing. **M. Benés:** Data curation. **A. de Goñi:** Data curation, Methodology. **B. Muñoz:** Data curation, Methodology. **M.U. Alzueta:** Conceptualization, Supervision, Writing - review & editing.

Declaration of Competing Interest

The authors declare that they have no known competing financial interests or personal relationships that could have appeared to influence the work reported in this paper.

Acknowledgements

The authors express their gratitude to the Aragón Government (Ref. T22_17R), co-funded by FEDER 2014-2020 "Construyendo Europa desde Aragón", and to MCIU and FEDER (Project RTI2018-098856-B-I00) for financial support.

Appendix A. Supplementary data

Supplementary data to this article can be found online at https://doi.org/10.1016/j.fuel.2021.120979.

References

[1] Valera-Medina A, Morris S, Runyon J, Pugh DG, Marsh R, Beasley P, et al. Ammonia, methane and hydrogen for gas turbines. Energy Procedia 2015;75:118–23.
[2] Valera-Medina A, Xiao H, Owen-Jones M, David WIF, Bowen PJ. Ammonia for power. Prog. Energy Combust. Sci. 2018;69:63–102.
[3] Kobayashi H, Hayakawa A, Kunkuma KD, Somarathne A, Okafor EC. Science and technology of ammonia combustion. Proc. Combust. Inst. 2019;37:109–33.
[4] Duynslaegher C, Jeanmart H, Vandooren J. Flame structure studies of premixed ammonia/hydrogen/oxygen/argon flames: Experimental and numerical investigation. Proc. Combust. Inst. 2009;32:1277–84.
[5] Tian Z, Li Y, Zhang L, Glarborg P, Qi F. An experimental and kinetic modeling study of premixed NH3/CH4/O2/Ar flames at low pressure. Combust. Flame 2009;156:1413–26.
[6] Hayakawa A, Goto T, Mimoto R, Kudo T, Kobayashi H. NO formation/reduction mechanisms of ammonia/air premixed flames at various equivalence ratios and pressures. Mech. Eng. J. 2015; 2:1 UNSP 14-00402.
[7] Hayakawa A, Goto T, Mimoto R, Arakawa Y, Kudo T, Kobayashi H. Laminar burning velocity and Markstein length of ammonia/air premixed flames at various pressures. Fuel 2015;159:98–106.
[8] Xiao H, Valera-Medina A, Bowen PJ. Study on premixed combustion characteristics of co-firing ammonia/methane fuels. Energy 2017;140:125–35.
[9] Han XL, Wang ZH, Costa M, Sun ZW, He Y, Cen KF. Experimental and kinetic modeling study of laminar burning velocities of NH_3/air, NH_3/H_2/air, NH_3/CO/air and NH_3/CH_4/air premixed flames. Combust. Flame 2019;206:214–26.
[10] Bull DC. A shock tube study of the oxidation of ammonia. Combust. Flame 1968;12:603–10.
[11] Mathieu O, Petersen EL. Experimental and modeling study on the high-temperature oxidation of ammonia and related NO_x chemistry. Combust. Flame 2015;162:554–70.
[12] Shu B, Vallabhuni SK, He X, Issayev G, Moshammer K, Farooq A, et al. A shock tube and modeling study on the autoignition properties of ammonia at intermediate temperatures. Proc. Combust. Inst. 2019;37:205–11.
[13] Pochet M, Dias V, Moreau B, Foucher F, Jeanmart H, Contino F. Experimental and numerical study, under LTC conditions, of ammonia ignition delay with and without hydrogen addition. Proc. Combust. Inst. 2019;37:621–9.
[14] Manna MV, Sabia P, Ragucci R, de Joannon M. Oxidation and pyrolysis of ammonia mixtures in model reactors. Fuel 2020;264:116768.
[15] Stagni A, Cavalloti C, Arunthanayothin S, Song Y, Herbinet O, Battin-Leclerck F, et al. An experimental, theoretical and kinetic-modeling study of the gas-phase oxidation of ammonia. React. Chem. Eng. 2020;5:696–711.
[16] Skreiberg Ø, Kilpinen P, Glarborg P. Ammonia chemistry below 1400 K under fuel-rich conditions in a flow reactor. Combust. Flame 2004;136:501–18.
[17] Song Y, Hashemi H, Christensen JM, Zhou C, Marshall P, Glarborg P. Ammonia oxidation at high pressure and intermediate temperatures. Fuel 2016;181:358–65.
[18] Bowman CT. Control of combustion-generated nitrogen oxide emissions: technology driven by regulation. Proc. Combust. Inst. 1992;24:859–78.
[19] Hasegawa T, Sato M. Study of ammonia removal from coal-gasified fuel. Combust. Flame 1998;114:246–58.
[20] Duynslaegher C, Contino F, Vandooren J, Jeanmart H. Modeling of ammonia combustion at low pressure. Combust. Flame 2012;159:2799–805.
[21] Okafor EC, Naito Y, Colson S, Ichikawa A, Kudo T, Hayakawa A, et al. Experimental and numerical study of the laminar burning velocity of CH_4-NH_3-air premixed flames. Combust Flame 2018;187:185–98.
[22] Otomo J, Koshi M, Mitsumori T, Iwasaki H, Yamada K. Chemical kinetic modeling of ammonia oxidation with improved reaction mechanism for ammonia/air and ammonia/hydrogen/air combustion. Int J Hydrogen Energy 2018;43:3004–14.
[23] Glarborg P, Miller JA, Ruscic B, Klippenstein SJ. Modeling nitrogen chemistry in combustion. Prog. Energy Combust. Sci. 2018;67:31–68.
[24] Klippenstein SJ, Pfeifle M, Jasper AW, Glarborg P. Theory and modeling of relevance to prompt-NO formation at high pressure. Combust. Flame 2018;195:3–17.
[25] Shrestha KP, Seidel L, Zeuch T, Mauss F. Detailed kinetic mechanism for the oxidation of ammonia including the formation and reduction of nitrogen oxides. Energy Fuel 2018;32:10202–17.
[26] Dai L, Gersen S, Glarborg P, Levinsky H. Experimental and numerical analysis of the autoignition behavior of NH_3 and NH_3/H_2 mixtures at high pressure. Combust. Flame 2020;215:134–44.
[27] Alzueta MU, Guerrero M, Millera A, Marshall P, Glarborg P. Experimental and kinetic modeling study of oxidation of acetonitrile. Proc. Combust. Inst. 2021;38:575–83.
[28] Abián M, Giménez-López J, Bilbao R, Alzueta MU. Effect of different concentration levels of CO_2 and H_2O on the oxidation of CO: experiments and modeling. Proc. Combust. Inst. 2011;33:317–23.
[29] Colom-Díaz JM, Abián JM, Ballester MY, Millera A, Bilbao R, Alzueta MU. H_2S conversion in a tubular flow reactor: Experiments and kinetic modeling. Proc. Combust. Inst. 2019;7:727–34.
[30] Alzueta MU, Glarborg P, Dam-Johansen K. Low temperature interactions between hydrocarbons and nitric oxide: an experimental study. Combust. Flame 1997;109:25–36.
[31] Dove JE, Nip WS. Shock-tube study of ammonia pyrolysis. Can. J. Chem. 1979;57:689–701.
[32] Konnov A, De Ruyck J. Kinetic modeling of the thermal decomposition of ammonia. Combust. Sci. Technol. 2000;152:23–37.
[33] Davidson DF, Köhse-Höinghaus K, Chang AY, Hanson RK. A pyrolysis mechanism for ammonia. Int. J. Chem. Kin. 1990;22:513–35.
[34] Hashemi H, Christensen JM, Gersen S, Levinsky H, Klippenstein SJ, Glarborg P. High-pressure oxidation of methane. Combust. Flame 2016;172:349–64.
[35] Hashemi H, Jacobsen JG, Rasmussen CT, Christensen JM, Glarborg P, Gersen S, et al. High-pressure oxidation of ethane. Combust. Flame 2017;182:150–66.
[36] Giménez-López J, Rasmussen CT, Hashemi H, Alzueta MU, Gao Y, Marshall P, et al. Experimental and kinetic modeling study of C_2H_2 oxidation at high pressure. Int. J. Chem. Kinet. 2016;48:724–38.
[37] Klippenstein SJ, Harding LB, Glarborg P, Miller JA. The role of NNH in NO formation and control. Combust. Flame 2011;158:774–89.
[38] Dagaut P, Glarborg P, Alzueta MU. The oxidation of hydrogen cyanide and related chemistry. Prog. Energy Combust. Sci. 2008;34:1–46.
[39] Glarborg P, Alzueta MU, Dam-Johansen K, Miller JA. Kinetic modeling of hydrocarbon/nitric oxide interactions in a flow reactor. Combust. Flame 1998;115:1–27.
[40] Mendiara T, Glarborg P. Ammonia chemistry in oxy-fuel combustion of methane. Combust. Flame 2009;156:1937–49.
[41] Mendiara T, Glarborg P. NO reduction in oxy-fuel combustion of methane. Energy Fuel 2009;23:3565–72.
[42] CHEMKIN-PRO 15131. Reaction Design, 2013.
[43] Benés M, Pozo G, Abián M, Millera A, Bilbao R, Alzueta MU. Experimental study of the pyrolysis of NH3 under flow reactor conditions. Energy Fuel 2021;35:7193–200. https://doi.org/10.1021/acs.energyfuels.0c03387.
[44] Dean AM, Chou MS, Stern D. Kinetics of rich ammonia flames. Int. J. Chem. Kinet. 1984;16:633–53.
[45] Dasch CJ, Blint RJ. A mechanistic and experimental study of ammonia flames. Combust. Sci. Technol. 1984;41:223–44.